Genetic Network Analyzer: A Tool for the Qualitative Simulation of Genetic Regulatory Networks

Hidde de Jong, Johannes Geiselmann, Céline Hernandez, Michel Page

INRIA

INSTITUT NATIONAL DE RECHERCHE EN INFORMATIQUE ET EN AUTOMATIQUE

Genetic Network Analyzer: A Tool for the Qualitative Simulation of Genetic Regulatory Networks

Hidde de Jong — Johannes Geiselmann — Céline Hernandez — Michel Page

N° 4262

Septembre 2001

THÈME 3

ISSN 0249-6399 ISRN INRIA/RR--4261--FR+ENG

INRIA
RHÔNE-ALPES

Genetic Network Analyzer: A Tool for the Qualitative Simulation of Genetic Regulatory Networks

Hidde de Jong , Johannes Geiselmann* , Céline Hernandez , Michel Page

Thème 3 — Interaction homme-machine,
images, données, connaissances
Projet HELIX

Rapport de recherche n° 4262 — Septembre 2001 — 16 pages

Abstract: The study of genetic regulatory networks has received a major impetus from the recent development of experimental techniques allowing the measurement of spatiotemporal patterns of gene expression in a massively parallel way. This progress of experimental methods calls for the development of appropriate computer tools for the modeling and simulation of gene regulation processes. These tools should be able to deal with two major difficulties hampering modeling and simulation studies, viz. incomplete knowledge of the biochemical reaction mechanisms and the absence of quantitative information on kinetic parameters and molecular concentrations.

We present the Genetic Network Analyzer (GNA), a computer tool for the modeling and simulation of genetic regulatory networks. The tool is based on a qualitative simulation method that employs coarse-grained models of regulatory networks. The use of GNA is illustrated in a study of the network of genes and interactions regulating the initiation of sporulation in *Bacillus subtilis*.

Key-words: genetic regulatory networks, mathematical modeling, simulation, bioinformatics, sporulation, *B. subtilis*

* CERMO, Université Joseph Fourier, Grenoble

Unité de recherche INRIA Rhône-Alpes
655, avenue de l'Europe, 38330 Montbonnot-St-Martin (France)
Téléphone : +33 4 76 61 52 00 —Télécopie +33 4 76 61 52 52

Genetic Network Analyzer: Un Outil pour la Simulation Qualitative de Réseaux de Régulation Génique

Résumé : L'analyse des réseaux de régulation géniques est fortement stimulée par le développement récent des méthodes expérimentales permettant de mesurer en parallèle les profils spatio-temporels de l'expression génique. Pour tirer profit de ces progrès, il est nécessaire de développer des outils appropriés pour la modélisation et la simulation de processus de régulation génique. Ces outils doivent être capables de surmonter deux problèmes majeurs. D'une part, les mécanismes sous-jacents aux interactions du réseau ne sont pas bien connus. D'autre part, des informations quantitatives sur les paramètres caractérisant les interactions et les concentrations moléculaires sont rarement disponibles.

Nous présentons un logiciel pour la modélisation et la simulation de réseaux de régulation géniques, appelé Genetic Network Analyzer (GNA). Cet outil est basé sur une méthode de simulation qualitative utilisant des modèles de très agrégés. L'utilisation de GNA est illustrée par une étude du réseau des gènes et des interactions contrôlant l'initiation de la sporulation chez *Bacillus subtilis*.

Mots-clés : réseaux de régulation géniques, modélisation mathématique, simulation, bioinformatique, sporulation, *B. subtilis*

1 Introduction

It is now commonly accepted that most interesting properties of an organism emerge from the interactions between its genes, proteins, metabolites, and other constituents. This implies that, in order to understand the functioning of an organism, we need to elucidate the networks of interactions involved in gene regulation, metabolism, signal transduction, and other cellular and intercellular processes.

The study of *genetic regulatory networks* has taken a qualitative leap through the use of modern genomic techniques that allow the simultaneous measurement of the expression levels of all genes of an organism [15, 23]. In addition to experimental tools, formal methods for the *modeling* and *simulation* of gene regulation processes will be indispensable. As most networks of interest involve many genes connected through interlocking positive and negative feedback loops, an intuitive understanding of their dynamics is difficult to obtain and may lead to erroneous conclusions. Formal modeling and simulation methods, especially when supported by computer tools, allow the behavior of large and complex systems to be predicted in a systematic way [7, 16].

Modeling and simulation of genetic regulatory networks are currently hampered by two major difficulties [3]. First of all, the biochemical reaction mechanisms underlying regulatory interactions are usually not or incompletely known. This prevents the formulation of detailed models of the kinetics of a regulatory system, such as the models developed for the genetic switch controlling phage λ growth [17] or the feedback mechanisms regulating tryptophan synthesis in *E. coli* [26]. The first problem is aggravated by a second problem, namely the general absence of quantitative information on kinetic parameters and molecular concentrations. As a consequence, traditional methods for numerical analysis are difficult to apply.

In response to the above problems, several approaches based on coarse-grained and/or qualitative models of genetic regulatory networks have been proposed. Boolean network models [13, 30] and their generalizations [19, 35] discretize the possible states of activation of a gene, and describe the regulatory structure of the network in terms of Boolean or multi-valued logic. Related approximations of regulatory interactions underlie various classes of piecewise-linear differential equation (PLDE) models of genetic regulatory networks [9, 20, 29]. The PLDEs have mathematical properties that favor the qualitative analysis of the steady-state and transient behavior of regulatory systems. More generally, qualitative simulation methods [14] have been applied to the modeling and simulation of genetic regulatory networks described by means of qualitative abstractions of ordinary differential equations [11, 36].

We have developed a *qualitative simulation method* that achieves a synthesis of the above approaches [5, 6]. The method recasts the mathematical analysis of PLDE models of genetic regulatory networks in terms of formal concepts and algorithms developed within qualitative simulation. By tailoring the simulation method to a particular class of models, we avoid the severe upscaling problems often encountered in applications of qualitative simulation. The simulation method has been implemented in a publicly available computer tool, called the *Genetic Network Analyzer (GNA)*.

The aim of this paper is to present the computer tool and illustrate its use in the context of a regulatory network of biological interest, consisting of the genes and interactions regulating the initiation of sporulation in the Gram-positive soil bacterium *Bacillus subtilis* [10, 12]. Under conditions of nutrient deprivation, *B. subtilis* can decide not to divide and form a dormant, environmentally-resistant spore instead. The decision to either divide or sporulate is controlled by a complex network of interactions integrating various environmental, cell-cyle, and metabolic signals. We have simulated the sporulation network using a model constructed from published reports of experiments [4]. The simulations reveal that the salient features of the initiation of sporulation are reproduced, but that an additional interaction, hypothesized in the literature before, may be involved.

In the next section, we specify the differential equation models used to describe genetic regulatory networks, and we briefly summarize the working of the simulation algorithm. Section 3 discusses the implementation of the method, while section 4 illustrates the application of GNA in the case of the

initiation of sporulation in *B. subtilis*. The paper concludes with a discussion of the simulation tool and an outline of ideas for further work.

2 Qualitative simulation method

2.1 Differential equation models

The dynamics of a genetic regulatory network can be described by a class of differential equations suggested by Mestl *et al.* [20], extending ideas originally proposed by Glass and Kauffman [9]. The equations have the general form

$$\dot{x}_i = f_i(\boldsymbol{x}) - g_i(\boldsymbol{x})\, x_i, \quad x_i \geq 0,\ 1 \leq i \leq n, \tag{1}$$

where $\boldsymbol{x} = [x_1, \ldots, x_n]'$ is a vector of cellular protein concentrations. The *state equations* (1) define the rate of change of the concentration x_i as the difference of the rate of synthesis $f_i(\boldsymbol{x})$ and the rate of degradation $g_i(\boldsymbol{x})\, x_i$ of the protein. Constant input protein concentrations can be defined by setting $\dot{x}_i = 0$.

The function $f_i : \mathbb{R}^n_{\geq 0} \to \mathbb{R}_{\geq 0}$ is defined as

$$f_i(\boldsymbol{x}) = \sum_{l \in L} \kappa_{il}\, b_{il}(\boldsymbol{x}) \geq 0, \tag{2}$$

where $\kappa_{il} > 0$ is a rate parameter, $b_{il} : \mathbb{R}^n_{\geq 0} \to \{0, 1\}$ a *regulation function* defined in terms of step functions, and L a possibly empty set of indices of regulation functions. A regulation function $b_{il}()$ is the arithmetic equivalent of a Boolean function expressing the logic of gene regulation [25]. In the simplest case, $f_i(\boldsymbol{x}) = \kappa_i\, s^+(x_j, \theta_j)$, with

$$s^+(x_j, \theta_j) = \begin{cases} 1, & x_j > \theta_j, \\ 0, & x_j < \theta_j. \end{cases}$$

The function says that below a threshold concentration $\theta_j > 0$ gene i is not expressed, whereas above this threshold it is expressed at a rate κ_i. If protein J is a negative regulator of gene i, we have $f_i(\boldsymbol{x}) = \kappa_i\, s^-(x_j, \theta_j)$, with $s^-(x_j, \theta_j) = 1 - s^+(x_j, \theta_j)$. More complex regulation functions can express the combined effects of several regulatory proteins (section 4).

The function $g_i()$ allows the regulation of protein degradation to be modeled. The function is defined analogously to (2), except that we demand that $g_i(\boldsymbol{x})$ is strictly positive. In addition, in order to formally distinguish degradation rates from synthesis rates, we will denote the former by γ instead of κ. Notice that with the above definitions of $f_i()$ and $g_i()$, the state equations (1) are *piecewise-linear*.

In the absence of numerical values for the threshold and rate parameters in (1), it is not possible to numerically simulate the behavior of a genetic regulatory network. Instead of precise numerical values, we specify qualitative constraints on the parameter values that can usually be inferred from biological data. These constraints, having the form of algebraic inequalities between parameters, are exploited by the simulation method to predict the qualitative dynamics of the regulatory system.

In general, a protein encoded by a gene will be involved in different interactions at different threshold concentrations. We can order the p_i threshold concentrations of gene i, yielding the *threshold inequalities*

$$0 < \theta_{i1} < \ldots < \theta_{i,p_i} < max_i. \tag{3}$$

The parameter max_i denotes a maximum concentration for the protein encoded by gene i.

The $n-1$-dimensional threshold hyperplanes $x_i = \theta_{i,k_i}$, $1 \leq k_i \leq p_i$, divide the phase space into rectangular regions, so called *regulatory domains* [20]. Within each regulatory domain, the step

function expressions in (2) evaluate to 0 or 1, and hence $f_i()$ and $g_i()$ reduce to (sums of) rate constants. More precisely, $f_i()$ simplifies to some $\mu_i \in M_i \equiv \{f_i(\boldsymbol{x}) \mid \mathbf{0} \leq \boldsymbol{x} \leq \boldsymbol{max}\}$, and $g_i()$ to some $\nu_i \in N_i \equiv \{g_i(\boldsymbol{x}) \mid \mathbf{0} \leq \boldsymbol{x} \leq \boldsymbol{max}\}$. The sets M_i and N_i collect the different synthesis and degradation rates of the protein in different domains of the phase space.

It can be easily shown that all trajectories in a regulatory domain monotonically tend towards a single, stable steady state $\boldsymbol{x}^* = \boldsymbol{\mu}/\boldsymbol{\nu}$, the *target equilibrium*, lying at the intersection of the n hyperplanes $x_i = \mu_i/\nu_i$ [9, 20, 29]. The target equilibrium level μ_i/ν_i of the protein concentration x_i gives an indication of the strength of gene expression in the domain.

As in the case of threshold parameters, exact numerical values for the rate constants $\boldsymbol{\kappa}$ and $\boldsymbol{\gamma}$ are usually not available. However, biological data often does allow the possible target equilibrium levels of x_i^* in different regulatory domains to be ordered with respect to the threshold concentrations. The resulting *equilibrium inequalities* define the strength of gene expression in a regulatory domain in a qualitative way, on the scale of ordered threshold concentrations. More precisely, for every $\mu_i \in M_i$, $\nu_i \in N_i$, we specify some l_i, $1 \leq l_i < p_i$, such that

$$\theta_{i,l_i} < \mu_i/\nu_i < \theta_{i,l_i+1}, \tag{4}$$

or we set $0 < \mu_i/\nu_i < \theta_{i1}$ or $\theta_{i,p_i} < \mu_i/\nu_i < max_i$.

2.2 Qualitative simulation

In each regulatory domain, the system behaves in a qualitatively uniform way, in the sense that the solution trajectories monotonically approach a target equilibrium $\boldsymbol{x} = \boldsymbol{\mu}/\boldsymbol{\nu}$. As a consequence, each regulatory domain is associated with a *qualitative state* of the system, defined by a *qualitative value* for the concentration variable and its derivative [6]. The qualitative value for a concentration variable is given by the inequalities specifying the threshold bounds of the regulatory domain (e.g., $\theta_{i,k_i} < x_i < \theta_{i,k_i+1}$, for some k_i, $1 \leq k_i \leq p_i$). The qualitative value for the derivative of a concentration variable is given by the inequality specifying the sign pattern of the derivative in the regulatory domain (i.e., $\dot{x}_i < 0$, $\dot{x}_i > 0$, or $\dot{x}_i \lesseqgtr 0$, with $\dot{x}_i \lesseqgtr 0$ meaning that $\dot{x}_i < 0$, $\dot{x}_i = 0$, and $\dot{x}_i > 0$ in different parts of the domain).

With the above definitions, the basic idea of the *qualitative simulation* algorithm described in [6] can be summarized as follows. Given initial qualitative values $\boldsymbol{qv}_0$, describing the initial protein concentrations $\boldsymbol{x}$, the simulation algorithm computes the initial qualitative state qs_0, and then determines possible *transitions* from qs_0 to successor qualitative states that are consistent with the threshold and equilibrium inequalities. The generation of successor states is repeated in a recursive manner until all qualitative states reachable from the initial qualitative state have been found.

The qualitative states and transitions generated by the simulation algorithm form a *state transition graph*. The graph may contain cycles and states without successors, which are together referred to as *attractors*, and which may correspond to steady states and limit cycles of the differential equations (1) [9, 20, 29]. Since the number of possible qualitative states is finite, every path in the state transition graph will eventually reach an attractor. Each path running from the initial qualitative state qs_0 to an attractor forms a possible *qualitative behavior* of the regulatory system.

3 Genetic Network Analyzer (GNA)

The qualitative simulation method has been implemented in Java 1.3 in a program called *GNA (Genetic Network Analyzer)*. The graphical user interface *VisualGNA* assists the user in specifying the input of the simulator, controlling the simulation process, and analyzing the output (Fig. 1). GNA and VisualGNA can be downloaded from the authors' web site.

The simulation of a genetic regulatory network requires that the user specify a text file containing the state equations and the threshold and equilibrium inequalities. In addition, a text file with the

initial conditions must be provided. The syntax of the model and the initial conditions is defined by a Backus Naur Form (BNF) grammar which can be found in the GNA documentation. Fragments of the input files for the sporulation network are shown in App. A. A graphical model editor is currently under development.

A model describing a regulatory network can be selected by means of the Read Model option in the Model menu. GNA reads and parses the file, and from the resulting internal representation it generates a graphical display of the network. The user can choose between different algorithms to optimize the placement of the vertices and edges of the graph.

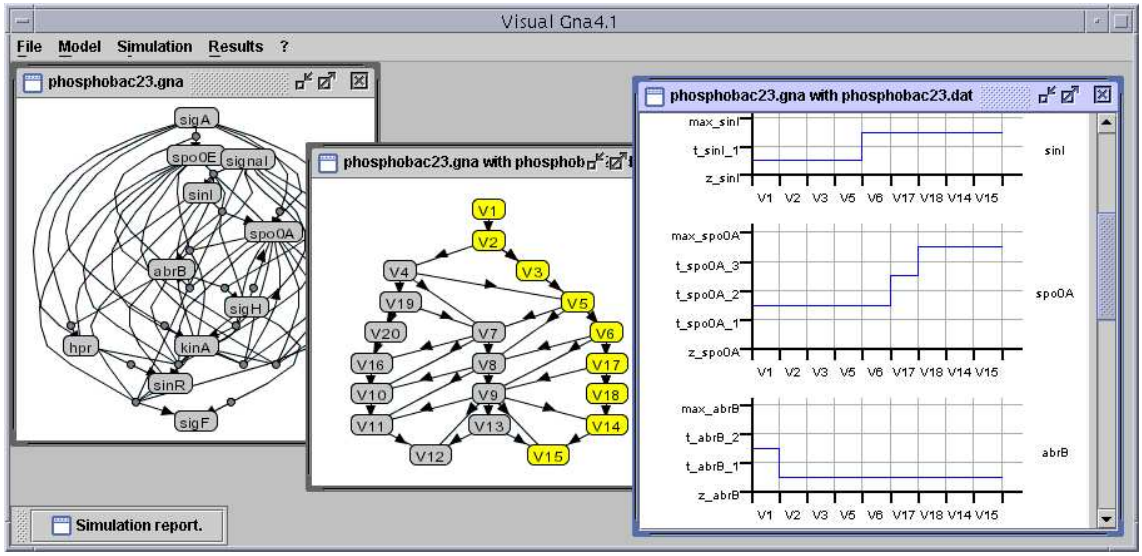

Figure 1: Modeling and simulation of a genetic regulatory network by means of GNA. The left window show the genes and interactions of the sporulation network, the middle window the state transition graph resulting from simulation of the network under initial conditions expected to induce sporulation, and the right window the temporal sequence of qualitative states in one selected path in the state transition graph.

A simulation can be started by choosing a file containing the initial conditions in the Simulation menu. The program determines in an iterative manner the state transitions that are possible from the specified initial conditions. This is achieved by an inequality reasoner tailored to the mathematical form of the state equations and parameter inequalities [5]. Alternatively, GNA can be instructed to perform a simulation for all possible initial conditions by means of the option Complete Analysis in the Simulation menu.

After completion of the simulation, GNA displays the state transition graph (Fig. 1). The attractors and their basins of attraction can be highlighted in the graph. By clicking on a sequence of states, partial and complete qualitative behaviors can be selected, and then studied in more detail by choosing the option Display States in the Results menu. The resulting chart shows how the qualitative state of the regulatory system changes over time in the selected behavior (Fig. 1).

4 Initiation of sporulation in *B. subtilis*

The use of the computer tool will be illustrated by modeling and simulating the regulatory network underlying the initiation of sporulation in *B. subtilis*. While nutrients are plentiful, *B. subtilis* divides as fast as possible in order to efficiently compete with its neighbors. However, when conditions become unfavorable, the bacterium protects itself by forming environmentally-resistant spores [10, 12, 31].

On the basis of the extensive literature on *B. subtilis* sporulation, and information contained in the database Subtilist [21], a model of the regulatory network controlling the initiation of sporulation has been constructed. A graphical representation of this network is shown in Fig. 2, displaying key genes and their promoters, proteins encoded by the genes, and the regulatory action of the proteins.

The network is centered around a phosphorylation pathway, the so-called *phosphorelay*, which integrates a variety of environmental, cell-cycle, and metabolic signals [10, 12]. Under conditions appropriate for sporulation, the phosphorelay transfers phosphates to the Spo0A regulator via a sequence of phosphorylation steps modulated by kinase and phosphatase proteins. The phosphorelay has been simplified in this paper by ignoring intermediate steps in the transfer of phosphate to Spo0A. However, this simplification does not affect the essential function of the phosphorelay: modulating the phosphate flux as a function of the competing action of kinases and phosphatases (here KinA and Spo0E) [24].

When input signals in favor of sporulation arrive, the concentration of Spo0A$\sim$P reaches a threshold value above which it activates various genes that commit the bacterium to sporulation. In order to produce a critical level of Spo0A$\sim$P, signals arriving at the phosphorelay need to be amplified and stabilized. This is achieved by a number of positive and negative feedback loops controlling the activity of the phosphorelay by transcriptional regulation of its components.

The decision to enter sporulation is thus not determined by a single gene, but emerging from a complex network of genes and regulatory interactions that integrates a variety of external stimuli. We have simulated this network to see whether salient features of the choice between vegetative growth and sporulation can be reproduced from the model [4].

4.1 Modeling of sporulation network

In order to model a genetic regulatory network, the functions $f_i(\boldsymbol{x})$ and $g_i(\boldsymbol{x})$ in (1) need to be defined. Recall from Sec. 2 that the functions are weighted step function expressions describing the regulatory logic of protein synthesis and degradation.

The use of step functions in gene regulation models has been motivated by the observation that the rate of activation of a gene, as a function of the concentration of a regulatory protein, often follows a steep sigmoidal curve [38]. That is, in the case of a repressor of transcription, below a certain threshold concentration of the protein, the gene will be maximally expressed, whereas above this threshold its expression rapidly falls down.

The use of step function approximations can be generalized to regulatory pathways in which proteins are modified through interactions with other proteins and small molecules. Consider the simplified phoshorelay, consisting of a phosphorylation/dephosphorylation cascade with Spo0A the substrate, KinA the protein kinase, and Spo0E the protein phosphatase. The product of the phosphorelay, Spo0A$\sim$P, activates the transcription of *abrB* [8, 32]. Analysis of a kinetic model of the simplified phosphorelay [28] shows that the rate of expression of *abrB* depends in a sigmoidal fashion on the total concentrations x_{sa} of Spo0A, x_{ka} of KinA, and x_{se} of Spo0E (Fig. 3).

In terms of step functions, the regulation of *spo0E*, a gene encoding a protein phosphatase involved in the phosphorelay, is described by

$$\dot{x}_{se} = \kappa_{se}\, s^-(x_{ab}, \theta_{ab_1})\, s^+(x_a, \theta_{a_1}) - \gamma_{se}\, x_{se}.$$

The differential equation states that *spo0E* is transcribed at a rate κ_{se} from a σ^A-promoter when the concentration x_{ab} of its repressor AbrB is below the threshold concentration θ_{ab_1} (i.e., $s^-(x_{ab}, \theta_{ab_1}) = 1$) [32]. In addition, for transcription to commence, the sigma factor σ^A encoded by *sigA* needs to be available at a concentration above the threshold θ_{sa_1} (i.e., $s^+(x_{sa}, \theta_{sa_1}) = 1$). Nothing is known about the regulation of Spo0E turnover; therefore a degradation rate proportional to the concentration of the protein has been assumed ($-\gamma_{se} x_{se}$).

The gene *abrB* is transcribed from two σ^A-promoters and is regulated by Spo0A$\sim$P and AbrB.

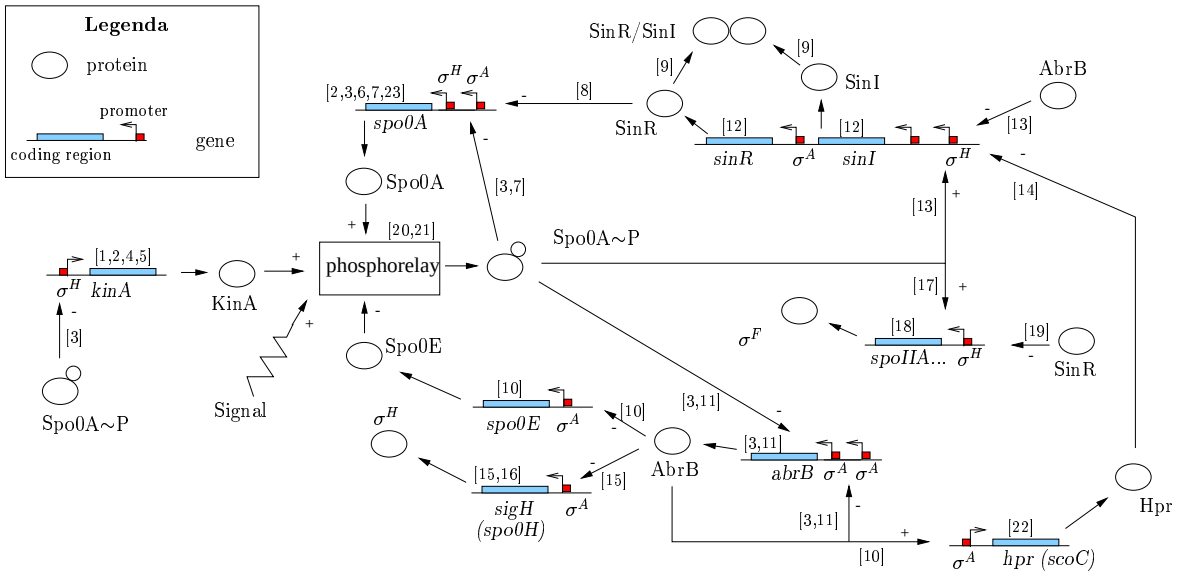

Figure 2: Genetic regulatory network underlying the inititation of sporulation in *B. subtilis*. For every gene, the coding region and the promoters are shown. Promoters are distinguished by the specific σ factor directing DNA transcription. The regulatory action of a protein tending to activate (inhibit) expression is indicated by a '+' ('-'). The numbers in the figure are references to the literature giving genetic and molecular evidence for the structure of the genes and for the regulatory interactions: [1] Jaacks *et al.* (1989), *J. Bacteriol.*, 171(8):4121; [2] Predich *et al.* (1992), *J. Bacteriol.*, 174(9):2771; [3] Fuyita and Sadaie (1998), *J. Biochem.*, 124:98; [4] LeDeaux *et al.* (1995), *J. Bacteriol.*, 177(3):861; [5] Jiang *et al.* (2000), *Mol. Microbiol.*, 38(3):535; [6] Chibazakura *et al.* (1991), *J. Bacteriol.*, 173(8):2625; [7] Strauch *et al.* (1992), *Biochimie*, 74:619; [8] Mandić-Mulic *et al.* (1995), *J. Bacteriol.*, 177(16):4619; [9] Bai and Mandić-Mulic (1993), *Genes Dev.*, 7:139; [10] Strauch *et al.* (1989), *EMBO J.*, 8(5):1615; [11] Strauch (1993), In: Sonenshein *et al.*, *Bacillus Subtilis and other Gram-Positive Bacteria*, ASM Press, 757; [12] Gaur *et al.* (1988), *J. Bacteriol.*, 170(3):1046; [13] Strauch and Hoch (1993), *Mol. Microbiol.*, 7(3):337; [14] Kallio *et al.* (1991), *J. Biol. Chem.*, 266(20):13411; [15] Weir *et al.* (1991), *J. Bacteriol.*, 173(2):521; [16] Healy *et al.* (1991), *Mol. Microbiol.*, 5(2):477; [17] Trach *et al.* (1991), *Res. Microbiol.*, 142:815; [18] Wu *et al.* (1991), *Gene*, 101(1):113; [19] Mandić-Mulic *et al.* (1992), *J. Bacteriol.*, 174(11):3561; [20] Burbulys *et al.* (1991), *Cell*, 64:545; [21] Hoch (1993), *Annu. Rev. Microbiol.*, 47:441; [22] Perego and Hoch (1988), *J. Bacteriol.*, 170(6):2560; [23] Yamashita *et al.* (1989), *J. Gen. Microbiol.*, 135:1335.

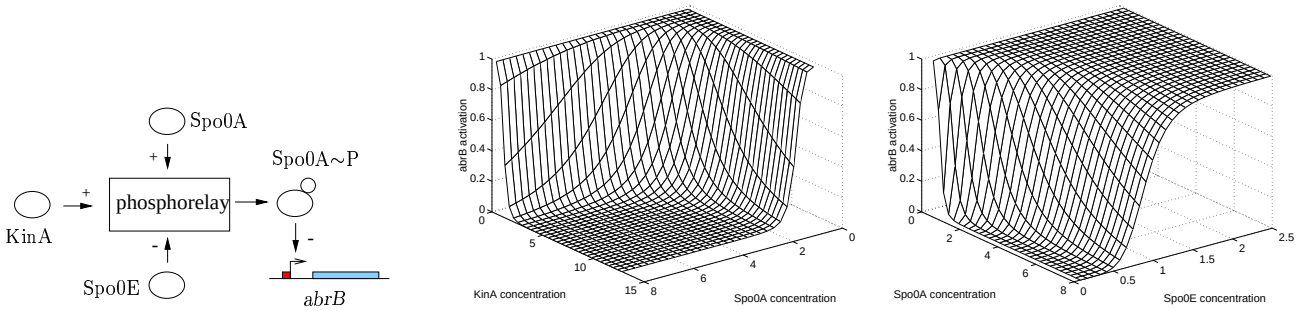

(a) (b) (c)

Figure 3: Sigmoidal regulation functions in gene regulation. (a) Repression of a target gene (*abrB*) by a phosphorylated regulatory protein (Spo0A∼P). The plots in (b)-(c) show expression of *abrB* as a function of the total concentration of the regulator (Spo0A), kinase (KinA), and phosphatase (Spo0E) in arbitrary units. In each plot, two of the concentrations are varied while the third is set to a constant value (the third plot has been omitted). The plots have been produced by solving the steady-state equation of the kinetic model in [28].

$$\dot{x}_{ab} = \kappa_{ab}\, s^-(x_{ab}, \theta_{ab_2})\, s^+(x_a, \theta_{a_1})\, (1 - s^+(x_{sa}, \theta_{sa_1})\, s^+(x_{ka}, \theta_{ka_1})\, s^-(x_{se}, \theta_{se_3})\, s^+(x_s, \theta_{s_1})) - \gamma_{ab}\, x_{ab}$$

abrB transcription is beginning to be inhibited at low concentrations of Spo0A∼P and at high concentrations of AbrB [8, 32]. As a consequence, for *abrB* to be transcribed at a rate κ_{ab}, the concentration of AbrB needs to be below the threshold θ_{ab_2} above which negative autoregulation takes place ($s^-(x_{ab}, \theta_{ab_2}) = 1$). Moreover, in the presence of the external signal, represented by $s^+(x_s, \theta_{s_1}) = 1$, the concentrations x_{sa} and x_{ka} of Spo0A and KinA must not lie above their respective thresholds θ_{sa_1} and θ_{ka_1} when the concentration x_{se} of Spo0E is below its threshold θ_{se_3}, since this would cause Spo0A∼P to attain a a level sufficient for shutting off *abrB* transcription ($1 - s^+(x_{sa}, \theta_{sa_1})\, s^+(x_{ka}, \theta_{ka_1})\, s^-(x_{se}, \theta_{se_3})\, s^+(x_s, \theta_{s_1}) = 1$). The degradation rate of AbrB equals $-\gamma_{ab} x_{ab}$.

AbrB has two threshold concentrations: θ_{ab_1} and θ_{ab_2}. The first threshold corresponds to the repression of *spo0E*, *sigH*, and other early sporulation genes by AbrB. Repression is lifted in stationary phase, when the AbrB concentration decreases [33]. The second threshold corresponds to the autoregulation of *abrB* during vegetative growth, when AbrB levels are at their highest. This motivates the folowing threshold inequalities for AbrB:

$$0 < \theta_{ab_1} < \theta_{ab_2} < max_{ab}.$$

Inspection of its state equation shows that x_{ab} will either tend to 0, in regions where the gene is repressed, or to κ_{ab}/γ_{ab}, in regions where the gene is transcribed at a rate κ_{ab}. The equilibrium level κ_{ab}/γ_{ab} is placed above the highest AbrB threshold, since otherwise the concentration of AbrB would never be able to reach or maintain a level at which negative autoregulation takes place. This leads to the equilibrium inequalities

$$\theta_{ab_2} < \kappa_{ab}/\gamma_{ab} < max_{ab}.$$

The state equations and parameter inequalities for the other proteins in the network of Fig. 2 have been constructed analogously (Fig. 4). The 10 state equations comprise a total of 45 step functions expressing the logic of gene regulation. For each of the proteins, 1 to 3 threshold concentrations and 1 to 3 equilibrium concentrations need to be ordered. Most of the time, the choice of appropriate parameter inequalities is strongly constrained by biological data. If the threshold and equilibrium

inequalities cannot be unambiguously determined on *a priori* grounds, they have been adjusted such that the model predictions match the observed behavior.

$\dot{x}_{ka} = \kappa_{ka_1} + \kappa_{ka_2}\,(1 - s^+(x_{sa},\theta_{sa_3})\,s^+(x_{ka},\theta_{ka_3})\,s^-(x_{se},\theta_{se_1})\,s^+(x_s,\theta_{s_1}))\,s^+(x_h,\theta_{h_1}) - \gamma_{ka}\,x_{ka}$ $0 < \theta_{ka_1} < \theta_{ka_2} < \theta_{ka_3} < max_{ka}$ $\theta_{ka_3} < (\kappa_{ka_1} + \kappa_{ka_2})/\gamma_{ka} < max_{ka},\ \ \theta_{ka_1} < \kappa_{ka_1}/\gamma_{ka} < \theta_{ka_2}$
$\dot{x}_h = \kappa_{h_1}\,s^-(x_{ab},\theta_{ab_1})\,s^+(x_a,\theta_{a_1}) - \gamma_h\,x_h$ $0 < \theta_{h_1} < max_h$ $\theta_{h_1} < \kappa_{h_1}/\gamma_h < max_h$
$\dot{x}_{se} = \kappa_{se_1}\,s^-(x_{ab},\theta_{ab_1})\,s^+(x_a,\theta_{a_1}) - \gamma_{se}\,x_{se}$ $0 < \theta_{se_1} < \theta_{se_2} < \theta_{se_3} < max_{se}$ $0 < \kappa_{se_1}/\gamma_{se} < \theta_{se_1}$
$\dot{x}_{ab} = \kappa_{ab_1}\,(1 - s^+(x_{sa},\theta_{sa_1})\,s^+(x_{ka},\theta_{ka_1})\,s^-(x_{se},\theta_{se_3})\,s^+(x_s,\theta_{s_1}))\,s^-(x_{ab},\theta_{ab_2})\,s^+(x_a,\theta_{a_1}) - \gamma_{ab}\,x_{ab}$ $0 < \theta_{ab_1} < \theta_{ab_2} < max_{ab}$ $\theta_{ab_2} < \kappa_{ab_1}/\gamma_{ab} < max_{ab}$
$\dot{x}_{sa} = \kappa_{sa_1}\,(1 - s^+(x_{sa},\theta_{sa_3})\,s^+(x_{ka},\theta_{ka_3})\,s^-(x_{se},\theta_{se_1})\,s^+(x_s,\theta_{s_1}))\,(1 - s^+(x_{sr},\theta_{sr_1})\,s^-(x_{si},\theta_{si_1}))\,s^+(x_h,\theta_{h_1})$ $\quad + \kappa_{sa_2}\,(1 - s^+(x_{sa},\theta_{sa_2})\,s^+(x_{ka},\theta_{ka_2})\,s^-(x_{se},\theta_{se_2})\,s^+(x_s,\theta_{s_1}))\,s^+(x_a,\theta_{a_1}) - \gamma_{sa}\,x_{sa}$ $0 < \theta_{sa_1} < \theta_{sa_2} < \theta_{sa_3} < max_{sa}$ $\theta_{sa_3} < \kappa_{sa_1}/\gamma_{sa} < max_{sa},\ \theta_{sa_1} < \kappa_{sa_2}/\gamma_{sa} < \theta_{sa_2},\ \ \theta_{sa_3} < (\kappa_{sa_1} + \kappa_{sa_2})/\gamma_{sa} < max_{sa}$
$\dot{x}_{si} = \kappa_{si_1}\,s^+(x_{sa},\theta_{sa_1})\,s^+(x_{ka},\theta_{ka_1})\,s^-(x_{se},\theta_{se_3})\,s^+(x_s,\theta_{s_1})\,s^-(x_{ab},\theta_{ab_1})\,s^-(x_{hr},\theta_{hr_1})\,s^+(x_h,\theta_{h_1}) - \gamma_{si}\,x_{si}$ $0 < \theta_{si_1} < max_{si}$ $\theta_{si_1} < \kappa_{si_1}/\gamma_{si} < max_{si}$
$\dot{x}_{sr} = \kappa_{sr_1}\,s^+(x_{sa},\theta_{sa_1})\,s^+(x_{ka},\theta_{ka_1})\,s^-(x_{se},\theta_{se_3})\,s^+(x_s,\theta_{s_1})\,s^-(x_{ab},\theta_{ab_1})\,s^-(x_{hr},\theta_{hr_1})\,s^+(x_h,\theta_{h_1}) + \kappa_{sr_2}\,s^+(x_a,\theta_{a_1})$ $\quad - \gamma_{sr}\,x_{sr}$ $0 < \theta_{sr_1} < max_{sr}$ $\theta_{sr_1} < \kappa_{sr_1}/\gamma_{sr} < max_{sr},\ \ \theta_{sr_1} < \kappa_{sr_2}/\gamma_{sr} < max_{sr},\ \theta_{sr_1} < (\kappa_{sr_1}) + \kappa_{sr_2})/\gamma_{sr} < max_{sr}$
$\dot{x}_{hr} = \kappa_{hr_1}\,s^+(x_{ab},\theta_{ab_1})\,s^+(x_a,\theta_{a_1}) - \gamma_{hr}\,x_{hr}$ $0 < \theta_{hr_1} < max_{hr}$ $\theta_{hr_1} < \kappa_{hr_1}/\gamma_{hr} < max_{hr}$
$\dot{x}_f = \kappa_{f_1}\,s^+(x_{sa},\theta_{sa_2})\,s^+(x_{ka},\theta_{ka_2})\,s^-(x_{se},\theta_{se_2})\,s^+(x_s,\theta_{s_1})\,(1 - s^+(x_{sr},\theta_{sr_1})\,s^-(x_{si},\theta_{si_1}))\,s^+(x_h,\theta_{h_1}) - \gamma_f\,x_f$ $0 < \theta_{f_1} < max_f$ $\theta_{f_1} < \kappa_{f_1}/\gamma_f < max_f$
$\dot{x}_a = 0$
$\dot{x}_s = 0$

Figure 4: State equations and parameter inequalities forming the model of the sporulation network discussed in Sec. 4. The model has nine state variables and one exogenous variable corresponding to the concentrations of key proteins. An additional exogenous variable denotes the presence of an external signal: x_{ka} (KinA), x_h (σ^H), x_{se} (Spo0E), x_{ab} (AbrB), x_{sa} (Spo0A), x_{si} (SinI), x_{sr} (SinR), x_{hr} (Hpr), x_f (σ^F), x_a (σ^A), x_s (signal).

4.2 Simulation of wild-type and mutant bacteria

GNA has been used to simulate the network underlying the initiation of sporulation from initial conditions reflecting a perturbation of the vegetative growth conditions. The perturbation consists in an external signal indicating a state of nutritional deprivation, which causes KinA to autophosphorylate ($s^+(x_s,\theta_{s_1}) = 1$).

Simulation of the network takes less than one second to complete on a SUN Ultra 10 workstation, and gives rise to a transition graph of 20 states, including two attractor states (Fig. 1). The attractor states both correspond to the decision of *B. subtilis* to enter sporulation, because σ^F, a transcription factor encoded by the *spoIIA* operon that is essential for the development of the forespore [31], is present above its threshold concentration θ_{f_1}.

Fig. 5(a) shows how the qualitative value of the proteins KinA, AbrB, Spo0A, and σ^F evolves in a typical behavior selected from the state transition graph. While the concentration of AbrB decreases as a consequence of the accumulation of Spo0A∼P, the concentrations of the phosphorelay components KinA and Spo0A increase, thus amplifying the flux of phosphate through the phosphorelay. The increase of the KinA and Spo0A concentrations is to be expected, as AbrB directly or indirectly represses their transcription (Fig. 2).

Much of what we know about the regulatory network underlying sporulation has come from the analysis of *B. subtilis* mutants [10]. Mutants can be modeled by adapting the differential equations in which the variable corresponding to the mutant gene occurs. A *sinI* mutant, for instance, gives rise to a state equation $\dot{x}_{si} = 0$, where x_{si} denotes the cellular concentration of SinI. Simulating the behavior of the *B. subtilis* mutant under sporulation conditions produces a transition graph with 9 qualitative states and a single attractor state corresponding to vegetative growth (Fig. 5(b)). That is, a *sinI* mutant is not expected to sporulate, an observation supported by biological data [1].

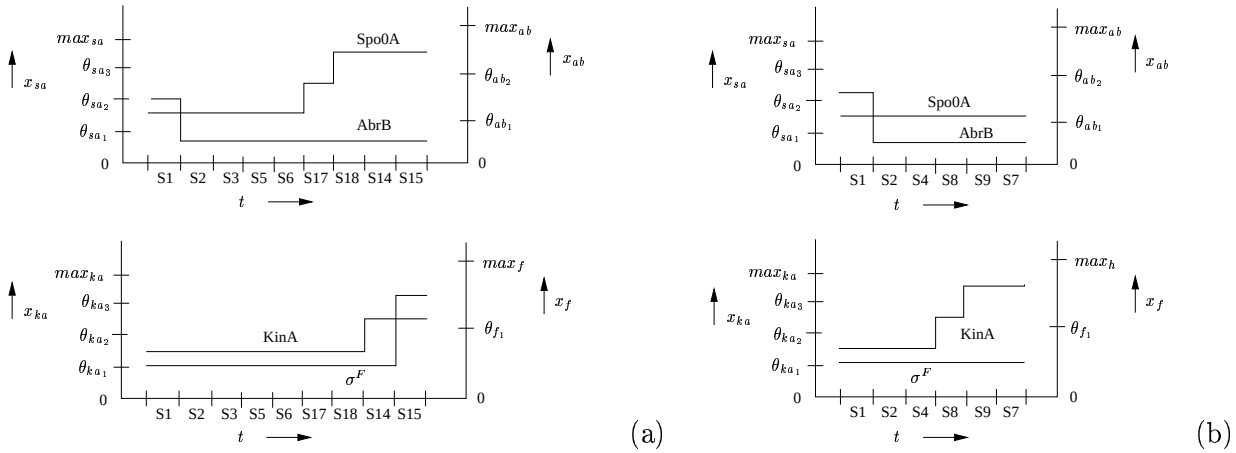

Figure 5: Results of the simulation of the network in Fig. 2 under conditions favoring sporulation. In (a) the results for a wild-type bacterium and in (b) the results for a *sinI*- mutant are shown. The graphs show the qualitative evolution of selected protein concentrations in a typical qualitative behavior in the state transition graph.

4.3 Analysis of simulation results

The simulated behavior of our network should reflect the essential biological characteristics of the sporulation initiation process. In particular, we expect to observe two types of attractor states, corresponding to vegetative growth and sporulation, and a controlled, all-or-non transition between these states in response to external stimuli [2].

Our model of the regulatory system reproduces exactly these properties. For a wide range of initial conditions, the simulations result in transition graphs with attractor states corresponding to vegetative growth (low concentrations of σ^H and Spo0A∼P, high concentration of AbrB) or sporulation (high concentrations of KinA and Spo0A∼P, activation of *spoIIA*). This tends to show that the connections within a biological system are such that almost all perturbations, even when they are contradictory, eventually return the system to a coherent pattern of gene activity representing a biological function or property.

A second important aspect of the model is that it shows how an external stimulus can lead to a transition from vegetative growth to sporulation. Low-amplitude signals from the environment are amplified and stabilized through feedback loops in order to provoke the change in the pattern of gene expression. When a cell in the vegetative growth phase receives a signal activating KinA, it will change its genetic program and induce sporulation. Our model of the network reproduces exactly this

behavior: turning the signal on in the vegetative growth state leads to amplification of the signal and conversion of the system to the sporulation state.

The available biological data on regulatory interactions constrain the topology of the core network to the connections shown in Fig. 2. In a similar way, biological data constrain the parameter inequalities. The (few) remaining freely adjustable orderings of threshold and equilibrium concentrations have been chosen so as to reproduce the observed behavior of the sporulating bacterium.

Analysis of the parameter inequalities thus obtained suggests that an interaction may be missing in the sporulation network of Fig. 2. In order to obtain results consistent with experimental data, we have to assume that the expression of *spo0E* is quite weak. That is, the target equilibrium concentrations of the Spo0E phosphatase have to be placed below its lower threshold concentrations ($0 < \kappa_{se}/\gamma_{se} < \theta_{se_1}$ and $\theta_{se_1} < \kappa_{se}/\gamma_{se} < \theta_{se_2}$). This is troublesome, because it implies that Spo0E cannot exert any influence on the decision to sporulate, as its concentration will not reach the threshold levels above which it can block the phosphate flux through the phosphorelay. As a remedy, we could postulate that an unknown signal decreases the activity of Spo0E at the onset of sporulation. Molecular studies of the interaction of Spo0E with components of the phosporelay suggest the existence of such a cellular factor which remains as of yet unidentified [22].

5 Discussion

We have presented a computer tool for the qualitative simulation of genetic regulatory networks and illustrated its use in the analysis of the network of interactions controlling the initiation of sporulation in *B. subtilis*. The computer tool implements a simulation method that is adapted to a class of ordinary differential equation models that are biologically valid and have been well-studied in mathematical biology [6]. Instead of numerical values, which are usually not available, qualitative constraints in the form of parameter inequalities are specified. Both the state equations and the parameter inequalities are obtained by directly translating biological data into a mathematical formalism.

Simulation of the sporulation network in Fig. 2 reveals that the essential features of the initiation of sporulation can be reproduced by means of a model constructed from the experimental literature. However, we also conclude that an additional interaction regulating the activity of the phosphatase Spo0E may be necessary for the decision to continue vegetative growth or to enter sporulation. This example demonstrates the potential of computer-supported modeling and simulation for discovering new and missing interactions and guide further experimentation.

Several computer tools for the simulation of biochemical reaction networks by means of differential equations are currently available [18, 27, 37]. GNA differs from these tools in an important respect: it has been developed for the qualitative instead of numerical simulation of one specific kind of networks, consisting of genes and their mutual regulatory interactions. The class of differential equations used to describe genetic regulatory networks has favorable mathematical properties that allow large and complex networks to be analyzed. GNA thus avoids the serious upscaling problems encountered by more general qualitative simulators like QSIM [14]. In comparison with the logical method of Thomas and colleagues [34, 35], which is based on comparable logical abstractions of regulatory interactions, GNA has been developed for differential equation models. We believe that the latter formalism is intuitively clear and of large generality. Moreover, it facilitates the integration of any quantitative data becoming available through modern genomic measurement technologies.

Upscaling is an important issue for modeling and simulation tools, since the behavioral properties of genetic regulatory networks emerge from the interactions among a large number of genes. Simulation of the sporulation network takes less than one second to complete on an average PC. Moreover, it turns out that of the 24576 possible qualitative states of the system only 20 are accessible from the initial state.

Even though the number of accessible states often forms a small proportion of the number of possible states, the exponential growth of the latter tends to make memory requirements the major

bottleneck for upscaling. Simulation experiments with random regulatory networks on a SUN Ultra 10 workstation with 128Mb of RAM have shown that the current version of GNA can simulate random regulatory networks involving up to 18 genes involved in complex feedback loops [5]. This number may be considerably larger in the case of real biological networks, which often have a redundant structure of interactions with robust behavioral properties.

The simulation tool produces gene expression profiles that can be directedly compared with experimental data obtained from quantitative RT-PCR and DNA microarrays. In fact, the qualitative predictions are well-adapted to the state-of-the-art measurement techniques in genomics, which are adequate for detecting qualitative changes in expression level, but usually lack quantitative precision. We are currently working on extensions of the method to validate and identify models of genetic regulatory networks using gene expression data. Incorporation of these extensions into GNA would allow the simulation tool to evolve into a more general tool for the computer-supported analysis of genetic regulatory networks.

Acknowledgments The authors would like to thank Gregory Batt, Sébastien Maza, Anne Morgat, Sébastien Provencher, François Rechenmann, Marie-France Sagot, Denis Thieffry, Ivayla Vatcheva, and Alain Viari for discussions and comments on a previous version of this paper.

References

[1] U. Bai and I. Mandić-Mulec. SinI modulates the activity of SinR, a developmental switch protein of *Bacillus subtilis*, by protein-protein interaction. *Genes & Development*, 7:139–148, 1993.

[2] J.D. Chung, G. Stephanopoulos, K. Ireton, and A.D. Grossman. Gene expression in single cells of *Bacillus subtilis*: Evidence that a threshold mechanism controls the initiation of sporulation. *Journal of Bacteriology*, 176(7):1977–1984, 1994.

[3] H. de Jong. Modeling and simulation of genetic regulatory systems: A literature review. *Journal of Computational Biology*, 2001.

[4] H. de Jong, J. Geiselmann, C. Hernandez, and M. Page. Qualitative simulation of the initiation of sporulation in *B. subtilis*. In L. Duret, C. Gaspin, and T. Schiex, editors, *Recueil des Actes des Journées Ouvertes Biologie Informatique Mathématiques, JOBIM 2001*, pages 187–194, Toulouse, 2001.

[5] H. de Jong and M. Page. Qualitative simulation of large and complex genetic regulatory systems. In W. Horn, editor, *Proceedings of the 14th European Conference on Artificial Intelligence, ECAI 2000*, pages 141–145, Amsterdam, 2000. IOS Press.

[6] H. de Jong, M. Page, C. Hernandez, and J. Geiselmann. Qualitative simulation of genetic regulatory networks: Method and application. In B. Nebel, editor, *Proceedings of the Seventeenth International Joint Conference on Artificial Intelligence, IJCAI-01*, pages 67–73, San Mateo, CA, 2001. Morgan Kaufmann.

[7] D. Endy and R. Brent. Modelling cellular behavior. *Nature*, 409:391–395, 2001.

[8] M. Fuyita and Y. Sadaie. Feedback loops involving Spo0A and AbrB in *in vitro* transcription of the genes involved in the initiation of sporulation in *Bacillus subtilis*. *Journal of Biochemistry*, 124:98–104, 1998.

[9] L. Glass and S.A. Kauffman. The logical analysis of continuous non-linear biochemical control networks. *Journal of Theoretical Biology*, 39:103–129, 1973.

[10] A.D. Grossman. Genetic networks controlling the initiation of sporulation and the development of genetic competence in *Bacillus subtilis*. *Annual Review of Genetics*, 29:477–508, 1995.

[11] K.R. Heidtke and S. Schulze-Kremer. Design and implementation of a qualitative simulation model of λ phage infection. *Bioinformatics*, 14(1):81–91, 1998.

[12] J.A. Hoch. Regulation of the phosphorelay and the initiation of sporulation in *Bacillus subtilis*. *Annual Review of Microbiology*, 47:441–465, 1993.

[13] S.A. Kauffman. *The Origins of Order: Self-Organization and Selection in Evolution*. Oxford University Press, New York, 1993.

[14] B. Kuipers. *Qualitative Reasoning: Modeling and Simulation with Incomplete Knowledge*. MIT Press, Cambridge, MA, 1994.

[15] D.J. Lockhart and E.A. Winzeler. Genomics, gene expression and DNA arrays. *Nature*, 405:827–836, 2000.

[16] H.H. McAdams and A. Arkin. Simulation of prokaryotic genetic circuits. *Annual Review of Biophysics and Biomolecular Structure*, 27:199–224, 1998.

[17] H.H. McAdams and L. Shapiro. Circuit simulation of genetic networks. *Science*, 269:650–656, 1995.

[18] P. Mendes. GEPASI: A software package for modelling the dynamics, steady states and control of biochemical and other systems. *Computer Applications in the Biosciences*, 9(5):563–571, 1993.

[19] L. Mendoza, D. Thieffry, and E.R. Alvarez-Buylla. Genetic control of flower morphogenesis in *Arabidopsis thaliana*: A logical analysis. *Bioinformatics*, 15(7-8):593–606, 1999.

[20] T. Mestl, E. Plahte, and S.W. Omholt. A mathematical framework for describing and analysing gene regulatory networks. *Journal of Theoretical Biology*, 176:291–300, 1995.

[21] I. Moszer, P. Glaser, and A. Danchin. SubtiList: A relational database for the *Bacillus subtilis* genome. *Microbiology*, 141:261–268, 1995.

[22] K.L. Ohlsen, J.K. Grimsley, and J.A. Hoch. Deactivation of the sporulation transcription factor Spo0A by the Spo0E protein phosphatase. *Proceedings of the National Academy of Sciences of the USA*, 91:1756–1760, 1994.

[23] A. Pandey and M. Mann. Proteomics to study genes and genomes. *Nature*, 405:837–846, 2000.

[24] M. Perego. Kinase-phosphatase competition regulates *Bacillus subtilis* development. *Trends in Microbiology*, 6(9):366–370, 1998.

[25] E. Plahte, T. Mestl, and S.W. Omholt. A methodological basis for description and analysis of systems with complex switch-like interactions. *Journal of Mathematical Biology*, 36:321–348, 1998.

[26] M. Santillán and M.C. Mackey. Dynamic regulation of the tryptophan operon: A modeling study and comparison with experimental data. *Proceedings of the National Academy of Sciences of the USA*, 98(4):1364–1369, 2001.

[27] H.M. Sauro. SCAMP: A general-purpose simulator and metabolic control analysis program. *Computer Applications in the Biosciences*, 9(4):441–450, 1993.

[28] E. Shacter, P.B. Chock, and E.R. Stadtman. Regulation through phosphorylation/dephosphorylation cascade systems. *Journal of Biological Chemistry*, 259(19):12252–12259, 1984.

[29] E.H. Snoussi. Qualitative dynamics of piecewise-linear differential equations: A discrete mapping approach. *Dynamics and Stability of Systems*, 4(3-4):189–207, 1989.

[30] R. Somogyi and C.A. Sniegoski. Modeling the complexity of genetic networks: Understanding multigenic and pleiotropic regulation. *Complexity*, 1(6):45–63, 1996.

[31] P. Stragier and R. Losick. Molecular genetics of *Bacillus subtilis*. *Annual Review of Genetics*, 30:297–341, 1996.

[32] M.A. Strauch. AbrB, a transition state regulator. In A.L. Sonenshein, J.A. Hoch, and R. Losick, editors, *Bacillus subtilis and other Gram-Positive Bacteria: Biochemistry, Physiology, and Molecular Genetics*, pages 757–764. American Society for Microbiology, Washington, DC, 1993.

[33] M.A. Strauch and J.A. Hoch. Transition-state regulators: Sentinels of *Bacillus subtilis* post-exponential gene expression. *Molecular Microbiology*, 7(3):337–342, 1993.

[34] D. Thieffry, M. Colet, and R. Thomas. Formalisation of regulatory nets: A logical method and its automatization. *Mathematical Modelling and Scientific Computing*, 2:144–151, 1993.

[35] R. Thomas and R. d'Ari. *Biological Feedback*. CRC Press, Boca Raton, FL, 1990.

[36] R.B. Trelease, R.A. Henderson, and J.B. Park. A qualitative process system for modeling NF-κB and AP-1 gene regulation in immune cell biology research. *Artifical Intelligence in Medicine*, 17:303–321, 1999.

[37] E.O. Voit. *Computational Analysis of Biochemical Systems : A Practical Guide for Biochemists and Molecular Biologists*. Cambridge University Press, Cambridge, 2000.

[38] G. Yagil and E. Yagil. On the relation between effector concentration and the rate of induced enzyme synthesis. *Biophysical Journal*, 11:11–27, 1971.

A GNA input files

The input of GNA consists of a file with the model description and a file with initial conditions. We show here an extract of the model file for the sporulation network in Fig. 1, with the declarations, state equations, and parameter inequalities concerning the state variable x_{ab} (concentration AbrB), and the file with initial conditions.

...

```
state-variable: abrB
  zero-parameter: z_abrB
  box-parameter: max_abrB
  production-parameters: k_abrB_1
  degradation-parameters: g_abrB
  threshold-parameters: t_abrB_1, t_abrB_2
  state-equation:
    d/dt abrB =
    k_abrB_1 * (1 - s+(spo0A, t_spo0A_1)
                  * s+(kinA, t_kinA_1)
                  * s-(spo0E, t_spo0E_3 )
                  * s+(signal, t_signal_1))
```

```
                  * s-(abrB, t_abrB_2)
     * s+(sigA, t_sigA_1)
  - g_abrB * abrB
  threshold-inequalities:
     t_abrB_1 < t_abrB_2;
  nullcline-inequalities:
     k_abrB_1 > g_abrB * t_abrB_2;
     k_abrB_1 < g_abrB * max_abrB;


   ...

initial-conditions:
  kinA > t_kinA_1; kinA < t_kinA_2;
  sigH >= z_sigH; sigH < t_sigH_1;
  spo0E >= z_spo0E; spo0E < t_spo0E_1;
  abrB > t_abrB_1; abrB < t_abrB_2;
  spo0A > t_spo0A_1; spo0A < t_spo0A_2;
  sinI >= z_sinI; sinI < t_sinI_1;
  sinR > t_sinR_1; sinR <= max_sinR;
  sigF >= z_sigF; sigF < t_sigF_1;
  sigA > t_sigA_1; sigA <= max_sigA;
  signal > t_signal_1; signal <= max_signal;
  hpr > t_hpr_1; hpr <= max_hpr;
```

Unité de recherche INRIA Rhône-Alpes
655, avenue de l'Europe - 38330 Montbonnot-St-Martin (France)

Unité de recherche INRIA Lorraine : LORIA, Technopôle de Nancy-Brabois - Campus scientifique
615, rue du Jardin Botanique - BP 101 - 54602 Villers-lès-Nancy Cedex (France)
Unité de recherche INRIA Rennes : IRISA, Campus universitaire de Beaulieu - 35042 Rennes Cedex (France)
Unité de recherche INRIA Rocquencourt : Domaine de Voluceau - Rocquencourt - BP 105 - 78153 Le Chesnay Cedex (France)
Unité de recherche INRIA Sophia Antipolis : 2004, route des Lucioles - BP 93 - 06902 Sophia Antipolis Cedex (France)

Éditeur
INRIA - Domaine de Voluceau - Rocquencourt, BP 105 - 78153 Le Chesnay Cedex (France)
http://www.inria.fr
ISSN 0249-6399